ChemPubSoc Europe

DOI: 10.1002/chem.201501974

CHEMISTRY
A European Journal
Communication

Supramolecular Chemistry

Metal–Organic Frameworks (MOFs) as Multivalent Materials: Size Control and Surface Functionalization by Monovalent Capping Ligands

Timon Rijnaarts, Raquel Mejia-Ariza, Richard J. M. Egberink, Wies van Roosmalen, and Jurriaan Huskens*[a]

Abstract: Control over particle size and composition are pivotal to tune the properties of metal organic frameworks (MOFs), for example, for biomedical applications. Particle-size control and functionalization of MIL-88A were achieved by using stoichiometric replacement of a small fraction of the divalent fumarate by monovalent capping ligands. A fluorine-capping ligand was used to quantify the surface coverage of capping ligand at the surface of MIL-88A. Size control at the nanoscale was achieved by using a monovalent carboxylic acid-functionalized poly(ethylene glycol) (PEG-COOH) ligand at different concentrations. Finally, a biotin–carboxylic acid capping ligand was used to functionalize MIL-88A to bind fluorescently labeled streptavidin as an example towards bioapplications.

Metal–organic frameworks (MOFs) or porous coordination polymers constitute a heavily investigated class of materials consisting of metal ions or clusters thereof, and multivalent organic linkers.[1] MOFs are crystalline materials with high porosities (with reports of up to 90% free volume) and large internal surface areas (over 4000 $m^2 g^{-1}$).[2] MOF pore sizes range from several Å up to tens of nanometers. MOF compositions can be readily tuned by varying the metal or the organic linker and by the ability to functionalize by grafting the organic linker during or after synthesis.[3] The resulting properties make these MOFs suitable for various applications such as catalysis,[4] gas sorption,[5] and drug delivery.[3,4,6]

In the field of biomedicine, there is the need for well-defined carriers of, for example, drugs or imaging agents, often in the form of nanoparticles.[3,7,8] To use nanosized MOFs for intravenous drug delivery,[9] different properties are required: biodegradability,[10] low toxicity,[8] tuning of the pore size to control the encapsulation of molecules, such as drugs,[11] gases,[12] metal nanoparticles,[13] and nucleic acids,[14] water dispersibility,[8] monodisperse particle size tunable to less than 200 nm,[8,15] and controllable composition and functionalization of the surface.[16] A general and versatile fabrication methodology is crucial to control the MOF particle size and the chemical and physical properties of the particles for introducing ligands, for example, for dispersibility or targeting, and to achieve colloidal and in vivo (bio)chemical stability.

In particular, the particle size is a limiting factor for intravenous administration, but also for other applications, such as for embedding MOFs in other material matrices, for example, polymers and nanosize control, is important. For that reason, the preparation of monodisperse, well-defined, reproducible, and stable nanoparticles has been investigated by using different methods, such as conventional hydrosolvothermal,[8,12a,17] reverse-phase microemulsions,[18] interfacial,[19] sonochemical,[17a,20] and microwave-assisted syntheses,[8,15c,17a,21] and spray drying.[22] Of particular interest is the coordination modulation method,[15a,17b,23] in which monovalent capping ligands are added to control the nucleation phase by serving as a stopper of the crystal growth to form nanoMOFs. But it should be noted that this method currently has been employed only with simple alkyl carboxylic acids and those in large excess. Currently, a molecular and physicochemical concept to quantitatively control the MOF particle size simultaneous with their outer functionalization by using low amounts of more complex and functional ligand molecules is lacking.

On the other hand, in the realm of supramolecular chemistry, the formation of supramolecular nanoparticles (SNPs)[24] is controlled by multivalent/monovalent competition between the building blocks. Variation of the stoichiometry of these building blocks is a simple and effective means to tune the size of SNPs in a controllable manner, as well as their surface chemistry. In this strategy, the monovalent building block by default ends up on the outside of the SNP, and therefore, the increase of its fraction at the expense of the multivalent, cross-linking building block present in the core leads to an increase of the total particle surface area and thus to a decrease of the average particle size. Important to note is that the success of this control by stoichiometry is in part due to the strong enthalpic driving forces for binding and the concomitant drive for saturation of sites. Even stronger enthalpies are commonly observed in MOF formation. To the best of our knowledge, multivalent/monovalent competition by variation of the stoi-

[a] *T. Rijnaarts,[+] R. Mejia-Ariza,[+] R. J. M. Egberink, Dr. W. van Roosmalen, Prof. Dr. J. Huskens*
Molecular NanoFabrication group, MESA Institute for Nanotechnology
University of Twente, P.O. Box 217, 7500 AE Enschede (The Netherlands)
Fax: (+31) 53489-4645
E-mail: J.Huskens@utwente.nl
Homepage: http://www.utwente.nl/tnw/mnf/

[+] *These authors contributed equally to this work.*

Supporting information for this article is available on the WWW under http://dx.doi.org/10.1002/chem.201501974.

chiometry of the building blocks without using an excess of material has not been used to date as a fabrication strategy in the synthesis of nanoMOFs. Such a method would allow the easy and direct introduction of more complex and functional capping ligands onto the surface of MOFs without multistep procedures and without using large amounts of these ligands.

Herein, we describe the synthesis of functionalized nanoMOFs as multivalent materials. We apply the concept of size control and surface functionalization in one pot by controlling the ratio between mono- and multivalent building blocks while maintaining a 1:1 stoichiometry between the binding groups. In the context of MOFs, the metal ions or secondary building units and the organic linkers are the multivalent building blocks, while a capping ligand that contains a single binding moiety of the same nature as the organic linker is the monovalent building block. Maintaining the stoichiometry enables the saturation of sites by the system. In contrast to the other coordination modulation methods, we do not employ a large excess of capping molecules, but rather replace only a small fraction of the organic linker by a monovalent ligand. To demonstrate this concept, we adapted the MIL-88A system using ferric chloride and fumaric acid as the multivalent building blocks and different monovalent carboxylates as the capping ligands to achieve surface functionalization, size control, and biomolecular functionalization.

Scheme 1 shows the concept of multivalent/monovalent competition in MOF synthesis. By substituting a small part of the multivalent bridging ligand (fumaric acid) for a monovalent carboxylate capping ligand while keeping the number of moles of carboxylate groups constant in the reaction mixture, we aim to control particle size and surface functionality. If saturation of metal sites is an important driving force, it is expected that the MOF particle size will decrease when minor quantities (up to a few percent) of capping ligand are introduced. The monovalent capping ligand effectively terminates the surface, which inhibits particle growth. The capping ligands used in this study are: 1) a fluorine-containing capping ligand (CF_3-cy-COOH; cy = cyclohexyl) to introduce an element (F) that can be detected both by bulk elemental analysis and the surface-sensitive X-ray photoelectron spectroscopy (XPS); 2) a poly(ethylene glycol) (PEG) capping ligand with a molecular weight of 2000 g mol^{-1} (PEG-COOH), which provides water solubility, to study the effect of molecular size and steric interactions between the capping ligands on MOF particle size; and 3) a biotin-capping ligand (biotin-COOH), which allows biofunctionalization by the coupling with streptavidin.

The iron(III) fumarate MOF MIL-88A has been synthesized according to an adapted microwave synthesis of Chalati et al.[17a] The synthesis yielded elongated particles (aspect ratio of 4.7) with a length of 1.70 ± 0.55 μm and a width of 0.36 ± 0.11 μm (Figure 1 a). Analysis by using X-ray diffraction (XRD), as well as transmission electron microscopy (TEM) and total reflection X-

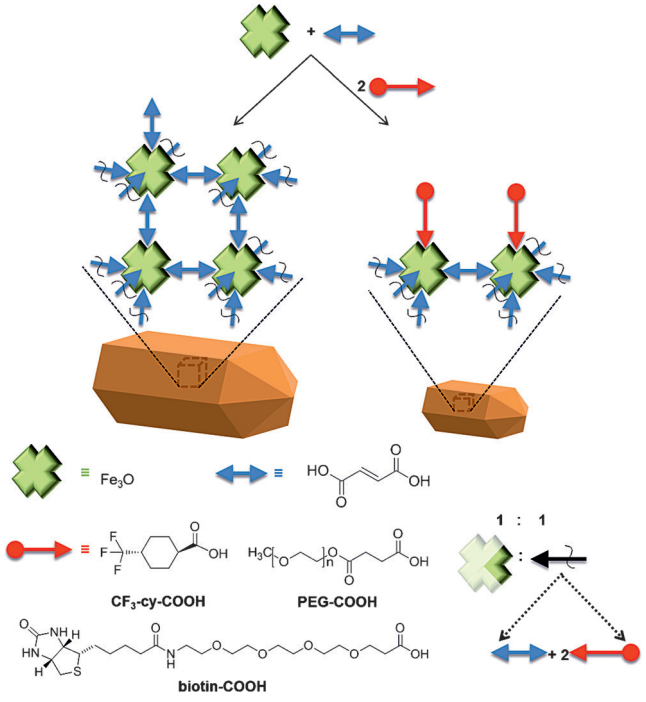

Scheme 1. Multivalent/monovalent competition in MOF synthesis: conceptual image of the introduction of monovalent capping ligands (red), which terminate the particle surface and thereby control the particle size.

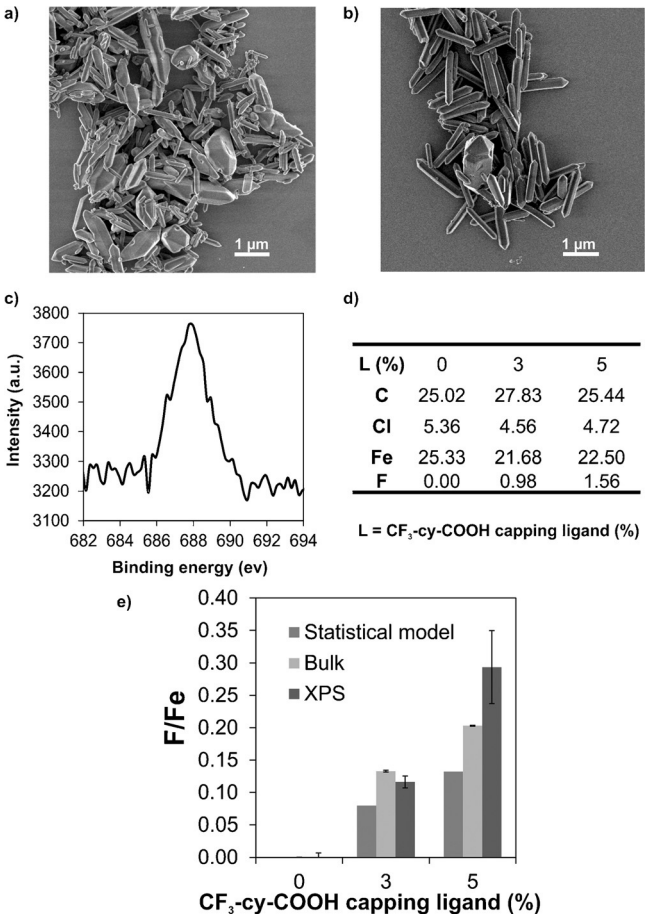

Figure 1. SEM images of MIL-88A with a) 0% and b) 3% CF_3-cy-COOH capping ligand; c) F1s XPS spectra for MIL-88A functionalized with 3% CF_3-cy-COOH capping ligand; d) elemental analyses (w%) of MIL-88A without and with CF_3-cy-COOH capping ligand and e) F/Fe atom% ratios using statistical composition, bulk elemental analysis, and XPS.

ray fluorescence (TXRF), confirmed the successful synthesis of MIL-88A (Figures S1, and S2 and Table S1 in the Supporting Information). Calculations of area and volume for MIL-88A (non-functionalized and functionalized particles) are given in the SI. Synthesis of MIL-88A functionalized with CF_3-cy-COOH was performed by substituting 1, 3, or 5% of fumaric acid for CF_3-cy-COOH (Figure 1b for a SEM image using 3% CF_3-cy-COOH). XRD experiments confirmed that all samples were crystalline MIL-88A (Figure S3 in the Supporting Information). Note that the powder XRD spectra patterns of the different MIL-88A differ from reported values due to differences in pore opening as a consequence of their flexible structure, their smaller size, and the effect of water absorption inside the pores, as was described before.[25] Additionally, as is shown below, a fraction of the F capping ligand is incorporated at a coordination site, which may cause some crystal damage leading to smaller crystallite sizes. Sorption experiments of MIL-88A gave a Brunauer–Emmett–and Teller (BET) surface area of 348 m^2g^{-1}, which is similar to previous results (see Figure S4 in the Supporting Information).[13a] However, upon addition of 1% of F capping ligand, the BET surface area decreased by 40%. This decrease in the presence of the F capping ligand is explained in three ways: 1) presence of the ligand at the surface can block the pore entrances; 2) binding of the ligand inside the lattice at a coordination site may cause crystal damage, smaller crystallite sizes and possible pore blockages; and 3) incorporation of the ligand as a counterion, loosely connected to the lattice, could lead to reduced accessibility.

XPS was used to analyze the surface elemental composition. Figure 1c shows the XPS F1s spectrum of the 3% ligand sample, qualitatively indicating the presence of F at the surface of the MOF particles. An increase in fluorine content was observed with increasing amount of capping ligand (Table S2 in the Supporting Information). Elemental analysis was used to analyze the bulk elemental composition (Figure 1d). The fluorine content was found to increase significantly whereas the chlorine content decreased slightly. To explain these trends, one has to look at the structure: MIL-88A is composed of Fe_3O inorganic building blocks, which are linked together by fumarate ligands. To obtain charge neutrality, one negative charge per Fe_3O unit is needed which is a chloride or negative monovalent capping ligand supplied from the synthesis mixture during preparation. In functionalized MIL-88A, the structure is $Fe_3O(OOC{-}C_2H_2{-}COO)_3Cl_z{\cdot}R{-}COO_{1-z}{\cdot}3H_2O$, in which R–COO is the monovalent capping ligand. Based on a statistical composition of these anions (chloride and capping ligand) by assuming equal probabilities for incorporation into the MOF crystal according to their presence in the synthesis solution, the value for z is calculated as 0.980 and 0.968 for 3% and 5% substitution, respectively, by the CF_3-cy-COOH capping ligand (see Equation S14 in the Supporting Information).

The Cl contents are in good agreement with the stoichiometric value of 0.33 for Cl/Fe, because one chloride anion should compensate for the charge of one Fe_3O block (Figure S5 in the Supporting Information). The decrease in chloride content in the MOF crystal upon increase of capping ligand is qualitatively observed as expected from the described statistical counterion model, but the experimental Cl/Fe ratio is not decreasing as much as the model predicts. This suggests that a small fraction of CF_3-cy-COOH capping ligand is inside the crystal as a counterion and an even smaller fraction possibly at a coordination site, causing a crystal defect.

For comparing the bulk and surface composition of the MOF, the ratio between fluorine (F) and iron (Fe) is used. In Figure 1e, the F/Fe atom% ratios are shown for increasing quantities of fluorine-capping ligand as was predicted by the statistical counterion model, and obtained from experimental data, bulk elemental analysis, and surface-specific XPS analysis. These results show that the MOF contains more fluor compared to statistical replacement of chloride counterion for both the bulk of the material, as well as the surface. This increase is tentatively attributed to population of the capping ligand at the MOF particle surface. For MIL-88A particles of the size observed herein, approximately 1.4% of the unit cells is located at the surface (see below), which can well explain the observed increase in bulk F content. With 5% of the CF_3-cy-COOH capping ligand, substantially enhanced fluor contents in XPS has been observed, indicating that the surface is the prominent position for the capping ligand (Figure S6 in the Supporting Information).

Relative surface densities of the capping ligand have been calculated (Equations S15 and 16 in the Supporting Information) by comparing the XPS data with a model for depth-dependent X-ray penetration and photoelectron emission. The model assumes full surface site saturation by CF_3-Cy-COOH and parameters for X-ray penetration have been given as well (Figure S7 in the Supporting Information). In this way we estimated a maximum F/Fe ratio (0.31–0.33) and compared this value to the ones obtained by XPS. Relative surface coverages of 15.3, 36.8, and 90.0% were estimated (Equation S16 in the Supporting Information) accordingly for the samples with 1, 3, and 5% CF_3-cy-COOH capping ligand, respectively (Table S3 in the Supporting Information).

As a next step, the effect of monovalent capping ligands on particle size and aspect ratio was studied by using the fluorinated ligand and a PEG-functionalized capping ligand. XRD experiments confirmed that all samples were crystalline MIL-88A (Figure S8 in the Supporting Information). For the fluorinated ligand, a significant particle-size effect was observed (Figures S9 and 10 in the Supporting Information). A statistical analysis (t test) on the data shown in Figure S10 in the Supporting Information (see Tables S4 and 5 in the Supporting Information) showed p values below 0.05 for both 0% versus 1%F and 0% versus 3%F for both length and width, all p are, indicating that the differences in particle length and width are significant for all comparisons. For the PEG ligand, the decrease in particle size was more pronounced, as was observed by a decrease of the length by a factor of two when using only 0.1% of PEG ligand (Figure 2a, b). Higher quantities of PEG-functionalized capping ligand induced an even stronger particle-size decrease, reaching lengths down to approximately 200 nm. Beyond 0.5% of PEG capping ligand (see SEM image in Figure 2c), the particle size did not decrease significantly anymore. The width of the PEG-capped particles is less affected as

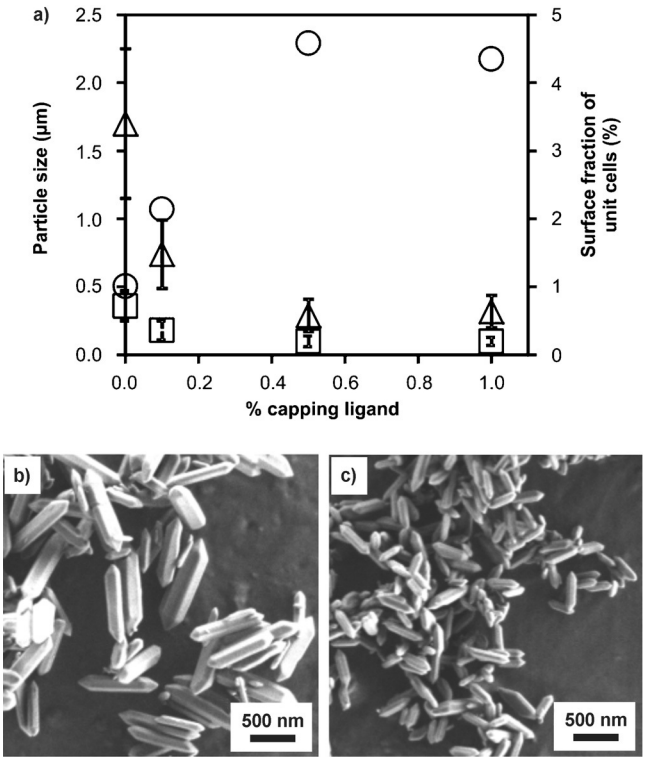

Figure 2. a) Particle length (left, triangles) and width (left, squares) and surface fraction of unit cells (%; right, circles) as a function of percentage PEG-COOH capping ligand. SEM images of MIL-88A with b) 0.1% and c) 0.5% PEG-COOH capping ligand.

witnessed by an aspect ratio of 3.1 compared to the standard MIL-88A particles (aspect ratio 4.8). Yet, the crystals retained their characteristic elongated shape and triangular faceted ends. The particle sizes using only 0.5% of PEG-COOH are similar to those reported earlier[8] when using 2% of PEG functionalized with amino groups, with similar size distributions.

The surface fraction of unit cells (defined as the number of unit cells at the surface versus the total number of unit cells, see the Supporting Information) increases if the particles become smaller. For the standard MIL-88A, 1.0% of the unit cells were at the surface. There is a remarkable difference between PEG- and CF_3-Cy-COOH-capped MIL-88A: the PEG-capped particles with only 0.5% substitution showed a significant increase in surface fraction of unit cells up to about 4.5% (Figure 2a). However, for CF_3-Cy-COOH-capped particles only a minor increase was observed up to 1.4% (Figure S11 in the Supporting Information). PEGs attached to surfaces can occupy a larger area, thus enhancing the capping effect compared to small capping ligands, and thereby apparently reduce the particle size more strongly. Elemental analysis of MIL-88A functionalized with 1% PEG-COOH showed that the %Cl decreased only slightly from 5.36 to 4.99 for 0 to 1% PEG-COOH, respectively, indicating no considerable uptake of the PEG-COOH in the bulk of the crystal (Table S6 in the Supporting Information). However, the BET surface area decreased strongly, compared with the F capping ligand to a value of 58.2 m^2g^{-1} (Figure S4 in the Supporting Information). These measurements show that the porosity is hampered to some extent by the outer functionalization; it appears thus to be dependent on the length of the outer ligand and compares well with earlier observed PEG-covered systems.[26]

Finally, to build a biomolecular system, MIL-88A was functionalized using biotin-containing capping ligand. This was achieved by substituting 1% of fumaric acid with biotin-COOH followed by binding of Alexa-Fluor488-streptavidin (Alexa-Fluor488-SAv). SEM imaging shows MIL-88A-biotin particles with a length of 1.50 ± 0.48 μm and a width of 0.13 ± 0.03 μm (Figure 3a). Additionally, analysis using XRD confirmed the successful synthesis of MIL-88A-biotin (Figure S12 in the Supporting Information). Upon incubation with Alexa-Fluor488-SAv, fluorescence imaging shows a strong fluorescence intensity demonstrating that biotin has been successfully bound to the MIL-88A surface and interacted with Alexa-Fluor488-SAv (Figure 3b). To test whether these interactions were specific, a control experiment was performed by mixing MIL-88A (without biotin) and Alexa-Fluor488-SAv (Figure 3c). As was expected, this led neither to any significant aggregation nor fluorescence due to the absence of biotin groups on the MOF surface.

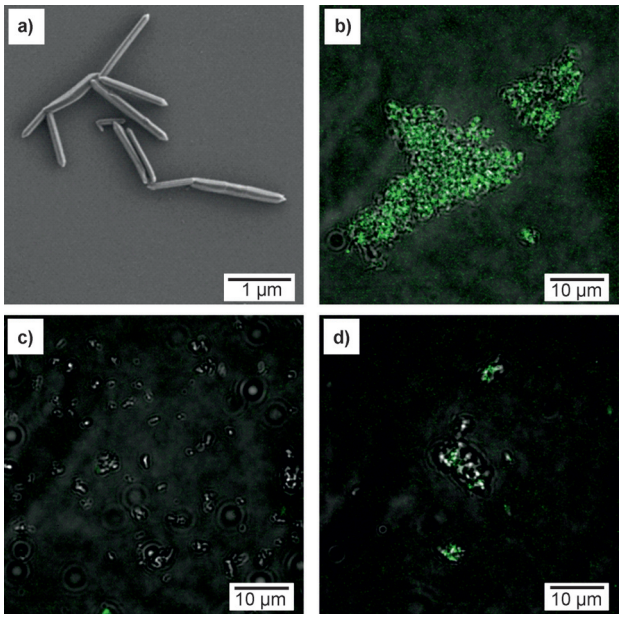

Figure 3. a) SEM image of MIL-88A-biotin and overlay images of optical and fluorescence confocal microscopy for b) MIL-88A-biotin after adsorption of Alexa-Fluor488-SAv, c) MIL-88A after adsorption of Alexa-Fluor488-SAv (control) and d) MIL-88A-biotin after adsorption of Alexa-Fluor488-SAv that was partially blocked with biotin (0.8 equiv).

Apart from the clear fluorescence of SAv, Figure 3b also shows strong aggregation of the MIL-88A-biotin particles upon incubation with SAv. This is attributed to the valency of the SAv: the protein has four identical binding pockets, which can induce cross-linking upon interaction with biotins of different particles. Also, this aggregation is promoted by the large ratio of biotin to SAv of 71.6 (see the Supporting Information for calculations). To suppress the aggregation, we pre-blocked SAv with free biotin before incubation with MIL-88A-biotin. Fluores-

cence imaging shows lower cluster formation even for 80% blocked SAv (Figure 3d). In addition, the fluorescence intensity for the blocked Alexa-Fluor488-SAv experiment was still higher than the blank (Figure S13 in the Supporting Information). In summary, these results showed that excluding multivalent specific interactions between MIL-88A-biotin and partially blocked SAv decreased the clustering while maintaining the specific interactions.

In conclusion, this work demonstrates the benefit of monovalent/multivalent competition under stoichiometric control by using a monovalent capping ligand, to simultaneously control the size and the functionalization of MIL-88A. The surface coverage of MIL-88A was assessed by using a capping ligand with fluorine, which allowed its quantitative analysis. Both small and large capping ligands significantly provide decrease of the MOF particle size. However, a larger capping ligand is more efficient due to its larger molecular size. Combination of these physicochemical properties make this MOF system a promising candidate for developing a targeting platform for biomolecules, such as proteins and nucleic acids and thus potentially for drug-delivery applications. For example, the herein shown biotin-MOFs may be tuned down in size into the nanoregime by straightforward use of the herein-developed concept, that is, by using biotin-PEG-COOH as a capping ligand. This well-controlled system will also be beneficial for other materials, such as polymer blends and other types of MOF systems.

Acknowledgements

This research was supported by the Council for Chemical Sciences of the Netherlands Organization for Scientific Research (NWO-CW, Vici grant 700.58.443 to J.H.). We gratefully thank Michael Holtkamp and Uwe Karst from the University of Münster for the TXRF measurements and Mikroanalytisches Laboratorium Kolbe for the elemental analysis. From the University of Twente: the Inorganic Material Science and Tissue Regeneration groups for the use of XRD apparatus and SEM imaging respectively, Cindy Huiskes from the Inorganic Membranes group for the BET experiments, Mark Smithers for TEM and HR-SEM imaging, and Gerard Kip for the XPS analysis.

Keywords: capping ligands · metal–organic frameworks · multivalent materials · nanoparticles · supramolecular chemistry

[1] A. K. Cheetham, C. N. R. Rao, *Science* **2007**, *318*, 58 – 59.
[2] S. Kitagawa, R. Kitaura, S.-i. Noro, *Angew. Chem. Int. Ed.* **2004**, *43*, 2334 – 2375; *Angew. Chem.* **2004**, *116*, 2388 – 2430.
[3] P. Horcajada, R. Gref, T. Baati, P. K. Allan, G. Maurin, P. Couvreur, G. Férey, R. E. Morris, C. Serre, *Chem. Rev.* **2011**, *111*, 1232 – 1268.
[4] R. J. Kuppler, D. J. Timmons, Q.-R. Fang, J.-R. Li, T. A. Makal, M. D. Young, D. Yuan, D. Zhao, W. Zhuang, H.-C. Zhou, *Coord. Chem. Rev.* **2009**, *253*, 3042 – 3066.
[5] A. U. Czaja, N. Trukhan, U. Muller, *Chem. Soc. Rev.* **2009**, *38*, 1284 – 1293.
[6] S. Keskin, S. Kızılel, *Ind. Eng. Chem. Res.* **2011**, *50*, 1799 – 1812.
[7] A. C. McKinlay, R. E. Morris, P. Horcajada, G. Férey, R. Gref, P. Couvreur, C. Serre, *Angew. Chem. Int. Ed.* **2010**, *49*, 6260 – 6266; *Angew. Chem.* **2010**, *122*, 6400 – 6406.
[8] P. Horcajada, T. Chalati, C. Serre, B. Gillet, C. Sebrie, T. Baati, J. F. Eubank, D. Heurtaux, P. Clayette, C. Kreuz, J.-S. Chang, Y. K. Hwang, V. Marsaud, P.-N. Bories, L. Cynober, S. Gil, G. Ferey, P. Couvreur, R. Gref, *Nat. Mater.* **2010**, *9*, 172 – 178.
[9] a) C. V. McGuire, R. S. Forgan, *Chem. Commun.* **2015**, *51*, 5199 – 5217; b) H. Furukawa, U. Müller, O. M. Yaghi, *Angew. Chem. Int. Ed.* **2015**, *54*, 3417 – 3430; *Angew. Chem.* **2015**, *127*, 3480 – 3494.
[10] S. R. Miller, D. Heurtaux, T. Baati, P. Horcajada, J.-M. Greneche, C. Serre, *Chem. Commun.* **2010**, *46*, 4526 – 4528.
[11] a) K. C. Stylianou, R. Heck, S. Y. Chong, J. Bacsa, J. T. A. Jones, Y. Z. Khimyak, D. Bradshaw, M. J. Rosseinsky, *J. Am. Chem. Soc.* **2010**, *132*, 4119 – 4130; b) J. Rabone, Y.-F. Yue, S. Y. Chong, K. C. Stylianou, J. Bacsa, D. Bradshaw, G. R. Darling, N. G. Berry, Y. Z. Khimyak, A. Y. Ganin, P. Wiper, J. B. Claridge, M. J. Rosseinsky, *Science* **2010**, *329*, 1053 – 1057; c) A. Mantion, L. Massüger, P. Rabu, C. Palivan, L. B. McCusker, A. Taubert, *J. Am. Chem. Soc.* **2008**, *130*, 2517 – 2526.
[12] a) L. J. Murray, M. Dinca, J. R. Long, *Chem. Soc. Rev.* **2009**, *38*, 1294 – 1314; b) K. Sumida, D. L. Rogow, J. A. Mason, T. M. McDonald, E. D. Bloch, Z. R. Herm, T.-H. Bae, J. R. Long, *Chem. Rev.* **2011**, *111*, 724 – 781; c) J.-R. Li, R. J. Kuppler, H.-C. Zhou, *Chem. Soc. Rev.* **2009**, *38*, 1477 – 1504.
[13] a) H. J. Lee, W. Cho, E. Lim, M. Oh, *Chem. Commun.* **2014**, *50*, 5476 – 5479; b) G. Lu, S. Li, Z. Guo, O. K. Farha, B. G. Hauser, X. Qi, Y. Wang, X. Wang, S. Han, X. Liu, J. S. DuChene, H. Zhang, Q. Zhang, X. Chen, J. Ma, S. C. J. Loo, W. D. Wei, Y. Yang, J. T. Hupp, F. Huo, *Nat. Chem.* **2012**, *4*, 310 – 316.
[14] W. Morris, W. E. Briley, E. Auyeung, M. D. Cabezas, C. A. Mirkin, *J. Am. Chem. Soc.* **2014**, *136*, 7261 – 7264.
[15] a) S. Hermes, T. Witte, T. Hikov, D. Zacher, S. Bahnmüller, G. Langstein, K. Huber, R. A. Fischer, *J. Am. Chem. Soc.* **2007**, *129*, 5324 – 5325; b) J. Cravillon, S. Münzer, S.-J. Lohmeier, A. Feldhoff, K. Huber, M. Wiebcke, *Chem. Mater.* **2009**, *21*, 1410 – 1412; c) Z. Ni, R. I. Masel, *J. Am. Chem. Soc.* **2006**, *128*, 12394 – 12395.
[16] a) M. D. Rowe, D. H. Thamm, S. L. Kraft, S. G. Boyes, *Biomacromolecules* **2009**, *10*, 983 – 993; b) M. D. Rowe, C.-C. Chang, D. H. Thamm, S. L. Kraft, J. F. Harmon, A. P. Vogt, B. S. Sumerlin, S. G. Boyes, *Langmuir* **2009**, *25*, 9487 – 9499.
[17] a) T. Chalati, P. Horcajada, R. Gref, P. Couvreur, C. Serre, *J. Mater. Chem.* **2011**, *21*, 2220 – 2227; b) W. Cho, H. J. Lee, M. Oh, *J. Am. Chem. Soc.* **2008**, *130*, 16943 – 16946; c) T. Tsuruoka, S. Furukawa, Y. Takashima, K. Yoshida, S. Isoda, S. Kitagawa, *Angew. Chem. Int. Ed.* **2009**, *48*, 4739 – 4743; *Angew. Chem.* **2009**, *121*, 4833 – 4837; d) N. Kerbellec, L. Catala, C. Daiguebonne, A. Gloter, O. Stephan, J.-C. Bunzli, O. Guillou, T. Mallah, *New J. Chem.* **2008**, *32*, 584 – 587.
[18] a) W. J. Rieter, K. M. L. Taylor, H. An, W. Lin, W. Lin, *J. Am. Chem. Soc.* **2006**, *128*, 9024 – 9025; b) K. M. L. Taylor, A. Jin, W. Lin, *Angew. Chem. Int. Ed.* **2008**, *47*, 7722 – 7725; *Angew. Chem.* **2008**, *120*, 7836 – 7839; c) W. J. Rieter, K. M. Pott, K. M. L. Taylor, W. Lin, *J. Am. Chem. Soc.* **2008**, *130*, 11584 – 11585; d) K. M. L. Taylor, W. J. Rieter, W. Lin, *J. Am. Chem. Soc.* **2008**, *130*, 14358 – 14359.
[19] R. Ameloot, F. Vermoortele, W. Vanhove, M. B. J. Roeffaers, B. F. Sels, D. E. De Vos, *Nat. Chem.* **2011**, *3*, 382 – 387.
[20] a) E. Haque, N. A. Khan, J. H. Park, S. H. Jhung, *Chem-Eur. J.* **2010**, *16*, 1046 – 1052; b) Z.-Q. Li, L.-G. Qiu, T. Xu, Y. Wu, W. Wang, Z.-Y. Wu, X. Jiang, *Mater. Lett.* **2009**, *63*, 78 – 80; c) L.-G. Qiu, Z.-Q. Li, Y. Wu, W. Wang, T. Xu, X. Jiang, *Chem. Commun.* **2008**, 3642 – 3644.
[21] G. A. Tompsett, W. C. Conner, K. S. Yngvesson, *ChemPhysChem* **2006**, *7*, 296 – 319.
[22] A. Carné-Sánchez, I. Imaz, M. Cano-Sarabia, D. Maspoch, *Nat. Chem.* **2013**, *5*, 203 – 211.
[23] a) H. Guo, Y. Zhu, S. Wang, S. Su, L. Zhou, H. Zhang, *Chem. Mater.* **2011**, *23*, 444 – 450; b) M. Ma, A. Gross, D. Zacher, A. Pinto, H. Noei, Y. Wang, R. A. Fischer, N. Metzler-Nolte, *CrystEngComm* **2011**, *13*, 2828 – 2832; c) D. Zacher, R. Nayuk, R. Schweins, R. A. Fischer, K. Huber, *Cryst. Growth Des.* **2014**, *14*, 4859 – 4863; d) A. Umemura, S. Diring, S. Furukawa, H. Uehara, T. Tsuruoka, S. Kitagawa, *J. Am. Chem. Soc.* **2011**, *133*, 15506 – 15513.
[24] a) H. Wang, S. Wang, H. Su, K.-J. Chen, A. L. Armijo, W.-Y. Lin, Y. Wang, J. Sun, K.-i. Kamei, J. Czernin, C. G. Radu, H.-R. Tseng, *Angew. Chem. Int. Ed.* **2009**, *48*, 4344 – 4348; *Angew. Chem.* **2009**, *121*, 4408 – 4412; b) H.

Wang, K.-J. Chen, S. Wang, M. Ohashi, K.-i. Kamei, J. Sun, J. H. Ha, K. Liu, H.-R. Tseng, *Chem. Commun.* **2010**, *46*, 1851 – 1853.

[25] a) P. Horcajada, F. Salles, S. Wuttke, T. Devic, D. Heurtaux, G. Maurin, A. Vimont, M. Daturi, O. David, E. Magnier, N. Stock, Y. Filinchuk, D. Popov, C. Riekel, G. Férey, C. Serre, *J. Am. Chem. Soc.* **2011**, *133*, 17839 – 17847; b) C. Tamames-Tabar, D. Cunha, E. Imbuluzqueta, F. Ragon, C. Serre, M. J. Blanco-Prieto, P. Horcajada, *J. Mater. Chem. B* **2014**, *2*, 262 – 271.

[26] V. Agostoni, P. Horcajada, M. Noiray, M. Malanga, A. Aykaç, L. Jicsinszky, A. Vargas-Berenguel, N. Semiramoth, S. Daoud-Mahammed, V. Nicolas, C. Martineau, F. Taulelle, J. Vigneron, A. Etcheberry, C. Serre, R. Gref, *Sci. Rep.* **2015**, *52*, 1 – 7.

Received: May 20, 2015
Published online on June 10, 2015